arXiv:1602.05202v3 [hep-ph] 1 Sep 2016

Pushing Higgs Effective Theory over the Edge

Anke Biekötter,[1] Johann Brehmer,[2] and Tilman Plehn[2]

[1] *Institut für Theoretische Teilchenphysik und Kosmologie, RWTH Aachen, Germany*
[2] *Institut für Theoretische Physik, Universität Heidelberg, Germany*

(Dated: September 2, 2016)

Based on a vector triplet model we study a possible failure of dimension-6 operators in describing LHC Higgs kinematics. First, we illustrate that including dimension-6 contributions squared can significantly improve the agreement between the full model and the dimension-6 approximation, both in associated Higgs production and in weak-boson-fusion Higgs production. Second, we test how a simplified model with an additional heavy scalar could improve the agreement in critical LHC observables. In weak boson fusion we find an improvement for virtuality-related observables at large energies, but at the cost of sizeable deviations in interference patterns and angular correlations.

CONTENTS

I. Introduction 2

II. To square or not to square 4
Higgs-strahlung 4
WBF Higgs production 5
Realistic tagging jets 10

III. Towards a simplified model 11
A pseudo-scalar as a simplified vector 12
Splitting functions and equivalence theorem 12
Which observable to study 14

IV. Summary 15

A. Effective scalar approximation 16

References 18

I. INTRODUCTION

After the discovery of a light Higgs boson [1, 2], one of the key tasks of the LHC is to test if the observed particle indeed corresponds to the minimalist setup of the Higgs sector in the Standard Model. Because of the many intricacies of the electroweak sector of the Standard Model, it is not straightforward to define a theoretical framework which describes possible deviations in the Higgs sector. If we want to remain more general than testing specific models [3], we can use an effective field theory ansatz. Here the Lagrangian is organized by the field or particle content, the symmetry structure, and the mass dimension [4–6].

The problem at least for the interpretation of Run I results in terms of an effective theory is the limited experimental accuracy. Combined with an assumed maximum size of underlying couplings the experimental precision determines the maximum testable hierarchy of scales [7, 8]. If for weakly interacting new physics models we assume that the higher-dimensional operators are ordered by factors $g^2 m_h^2/\Lambda^2$, or that the only relevant scale of Higgs production is given by m_h, a typical LHC accuracy of 10% on a rate measurement translates into a new physics reach around

$$\left| \frac{\sigma \times \text{BR}}{(\sigma \times \text{BR})_{\text{SM}}} - 1 \right| = \frac{g^2 m_h^2}{\Lambda^2} \gtrsim 10\% \qquad \Leftrightarrow \qquad \Lambda < \frac{g\, m_h}{\sqrt{10\%}} \approx 400 \text{ GeV} . \tag{1}$$

We assume $g < 1$, implying a reasonably weakly interacting theory, equivalent to Wilson coefficients of order one. This is exactly the Λ range we find in the full analysis [7].

This does *not* mean that an analysis of LHC data in terms of a truncated dimension-6 Lagrangian cannot be useful, but it does require us to carefully check the correspondence between the dimension-6 Lagrangian and complete models. It turns out that a dimension-6 Lagrangian describes weakly interacting extensions of the Higgs-gauge sector at the LHC well [9]. One key ingredient to this success is a v-improved matching procedure [9], which includes effects of the Higgs VEV in the matching to a Lagrangian with linearly realized electroweak symmetry breaking. The simplest realization of this idea is to set the new physics scale Λ to the physical mass of new particles including contributions from the Higgs VEV instead of using the mass scale in the unbroken phase of the electroweak symmetry. This effectively absorbs effects from dimension-8 operators into the dimension-6 Lagrangian by replacing $\phi^\dagger \phi \to v^2/2$. These terms are negligible when $v \ll \Lambda$, but can significantly improve the accuracy of the dimension-6 model in scenarios without a clear separation of scales [9].

This study rests on the findings of the more theoretical discussion in Ref. [9]. For models where that discussion does not lead to an obvious conclusion it attempts to answer two experimental key questions:

1. Is it justified or preferable to include dimension-6 operators squared while neglecting dimension-8 operators interfering with the Standard Model?

2. How can we improve our description when even the v-improved matching starts to fail and new states affect the LHC kinematics?

The first point is of immediate practical relevance for fits of Wilson coefficients to LHC data and has been discussed from different perspectives [7, 9–13].

These questions cannot be answered without making assumptions about the new physics scenario. We will illustrate them in a specific setup with a modified gauge sector [14], a setup known to challenge the dimension-6 framework [9]. We will rely on an extension of the Standard Model

HISZ basis		
$\mathcal{O}_{\phi 1} = (D_\mu \phi)^\dagger \, \phi \, \phi^\dagger \, (D^\mu \phi)$	$\mathcal{O}_{\phi 2} = \frac{1}{2} \partial^\mu (\phi^\dagger \phi) \, \partial_\mu (\phi^\dagger \phi)$	$\mathcal{O}_{\phi 3} = \frac{1}{3} (\phi^\dagger \, \phi)^3$
$\mathcal{O}_{GG} = (\phi^\dagger \, \phi) \, G^A_{\mu\nu} \, G^{\mu\nu \, A}$		
$\mathcal{O}_{BB} = -\frac{g'^2}{4} (\phi^\dagger \, \phi) \, B_{\mu\nu} \, B^{\mu\nu}$	$\mathcal{O}_{WW} = -\frac{g^2}{4} (\phi^\dagger \, \phi) \, W^k_{\mu\nu} \, W^{\mu\nu \, k}$	$\mathcal{O}_{BW} = -\frac{g \, g'}{4} (\phi^\dagger \sigma^k \phi) \, B_{\mu\nu} \, W^{\mu\nu \, k}$
$\mathcal{O}_B = \frac{ig}{2} (D^\mu \phi^\dagger)(D^\nu \phi) \, B_{\mu\nu}$	$\mathcal{O}_W = \frac{ig}{2} (D^\mu \phi^\dagger) \sigma^k (D^\nu \phi) \, W^k_{\mu\nu}$	
$\mathcal{O}_{u\phi} = (\phi^\dagger \phi)(\bar{Q}_3 \tilde{\phi} u_R)$	$\mathcal{O}_{d\phi} = (\phi^\dagger \phi)(\bar{Q}_3 \phi d_R)$	$\mathcal{O}_{e\phi} = (\phi^\dagger \phi)(\bar{L}_3 \phi e_R)$

Table I. Bosonic CP-conserving Higgs operators in the HISZ basis.

by a massive vector field $\tilde{V}^a_\mu$ which is a triplet under $SU(2)_L$ and has the mass $M_{\tilde{V}}$ [9, 15].* Its Lagrangian includes the terms

$$\begin{aligned} \mathcal{L} \supset & -\frac{1}{4} \tilde{V}^a_{\mu\nu} \tilde{V}^{\mu\nu \, a} + \frac{M^2_{\tilde{V}}}{2} \tilde{V}^a_\mu \tilde{V}^{\mu \, a} + i \frac{g_V}{2} c_H \tilde{V}^a_\mu \left[\phi^\dagger \sigma^a \overleftrightarrow{D}^\mu \phi \right] + \frac{g_w^2}{2 g_V} \tilde{V}^a_\mu \sum_{\text{SM fermions}} c_F \overline{F}_L \gamma^\mu \sigma^a F_L \\ & + \frac{g_V}{2} c_{VVV} \epsilon_{abc} \tilde{V}^a_\mu \tilde{V}^b_\nu D^{[\mu} \tilde{V}^{\nu] c} + g_V^2 c_{VVHH} \tilde{V}^a_\mu \tilde{V}^{\mu a} (\phi^\dagger \phi) - \frac{g_w}{2} c_{VVW} \epsilon_{abc} W^{\mu\nu} \tilde{V}^b_\mu \tilde{V}^c_\nu \, . \end{aligned} \tag{2}$$

Five coupling parameters c_j describe the different interactions of the new vector triplet to itself, the Standard Model fermions F, the Higgs doublet ϕ, and the $SU(2)_L$ field strength $W^{\mu\nu}$. The covariant derivative acts on the triplet as $D_\mu \tilde{V}^a_\nu = \partial_\mu \tilde{V}^a_\nu + g_V \epsilon^{abc} \tilde{V}^b_\mu \tilde{V}^c_\nu$. The coupling constant g_V is the characteristic strength of the heavy vector-mediated interactions, while g_w denotes the $SU(2)_L$ gauge coupling. After mixing they will combine to the observed weak gauge coupling. This mixing of the new heavy states with the weak bosons combined with the new, heavy resonances is what can lead to large effects at the LHC.

Unlike in Ref. [9] we now define our dimension-6 Lagrangian in the HISZ basis [16], to make our results compatible with the SFitter Run I legacy analysis of Ref. [7]:

$$\mathcal{L} \supset \sum_i \frac{f_i}{\Lambda^2} \mathcal{O}_i \, , \tag{3}$$

with the Higgs operators $\mathcal{O}_i$ defined in Tab. I. Our v-improved matching scale is $\Lambda = m_\xi$, the mass of the neutral heavy particle ξ^0 after mixing of the new V state with the Z boson. The dimension-6 Wilson coefficients for the triplet model read

$$\begin{aligned} f_{\phi 2} &= \frac{3}{4} \left(-2 \, c_F \, g^2 + c_H \, g_V^2 \right) , & f_{WW} &= c_F \, c_H \\ f_{\phi 3} &= -3\lambda \left(-2 \, c_F \, g^2 + c_H \, g_V^2 \right) , & f_{BW} &= c_F \, c_H \equiv f_{WW} \\ f_{f\phi} &= -\frac{1}{4} y_f \, c_H \left(-2 \, c_F \, g^2 + c_H \, g_V^2 \right) , & f_W &= -2 \, c_F \, c_H \, . \end{aligned} \tag{4}$$

Structurally, those dimension-6 operators are of two types,

$$\mathcal{O} \propto \frac{g^2 v^2}{\Lambda^2} \qquad \text{and} \qquad \mathcal{O} \propto \frac{g^2 \partial^2}{\Lambda^2} \, . \tag{5}$$

* Such a model is not manifestly renormalizable, but can be embedded in a UV-complete theory in which V acquires its mass through a Higgs mechanism [14].

The second type of operator, such as $\mathcal{O}_{WW}$, introduces a momentum dependence in the VVh interaction and thereby modifies kinematic distributions in Higgs-strahlung and weak-boson-fusion (WBF) Higgs production. Problems with our v-improved dimension-6 approximation for LHC kinematics typically occur through those operators. For two benchmark points introduced in Tab [9], which challenge the agreement between full model and dimension-6 approximation, we give the Wilson coefficients in Tab. II. The benchmark point T1 features constructive interference between the dimension-6 amplitudes and the SM in weak boson fusion and destructive interference in Vh production, while for T4 it is the other way around. In this paper we will again study two particularly sensitive observables, the m_{Vh} (or $p_{T,V}$) distribution in Higgs-strahlung and the $p_{T,j}$ distribution in weak boson fusion. In models with extended Higgs sectors the m_{hh} distribution in Higgs pair production would develop very similar features, including an s-channel resonance, but is experimentally less pressing [9, 17].

II. TO SQUARE OR NOT TO SQUARE

If we accept that a dimension-6 Lagrangian describing Higgs signatures at the LHC is not necessarily part of a consistent effective field theory, but rather a successful and reproducible parametrization of weakly interacting new physics, there exists no fundamental motivation [7, 9–13] to include or to not include the dimension-6 squared term in

$$|\mathcal{M}_{4+6}|^2 = |\mathcal{M}_4|^2 + 2\,\mathrm{Re}\mathcal{M}_4^*\mathcal{M}_6 \overset{?}{+} |\mathcal{M}_6|^2 \,. \tag{6}$$

A dimension-6 squared term of comparable or larger size than the interference term can appear in phase-space regions with a suppressed dimension-4 prediction, even when the EFT expansion in E/Λ holds and dimension-8 effects are negligible. In the absence of any first-principle reason how to treat this term, we need to test the different possibilities from a practical perspective.

Higgs-strahlung

We first analyze associated Vh production with $V = W^\pm, Z$ at 13 TeV LHC energy. To retain as much phase space as possible we only consider the parton-level process

$$pp \to Vh \tag{7}$$

simulated in `MadGraph` [18] without cuts or decays, see Fig. 1. It is easy to see where in phase space the effective theory breaks down: for on-shell outgoing Higgs and gauge bosons a large momentum flow through the Higgs operator can only be generated through the virtual s-channel propagator. We can directly test this in the observable m_{Vh} distribution, comparing the full model with the dimension-6 approach at large momentum flow.

Benchmark	Triplet model						Dimension-6 approximation				
	$M_{\tilde{V}}$	g_V	c_H	c_F	c_{VVHH}	m_ξ	$f_{\phi 2}$	$f_{\phi 3}$	f_{WW}	f_W	$f_{u\phi 33}$
T1	591	3.0	−0.47	−5.0	2.0	1200	0.00	0.00	2.45	−4.90	0.00
T4	1246	3.0	−0.50	3.0	−0.2	1200	2.64	−1.37	−1.56	3.12	−0.87

Table II. Benchmark points for the vector triplet model and matched Wilson coefficients for the dimension-6 model. All masses are given in GeV. Table from Ref. [9].

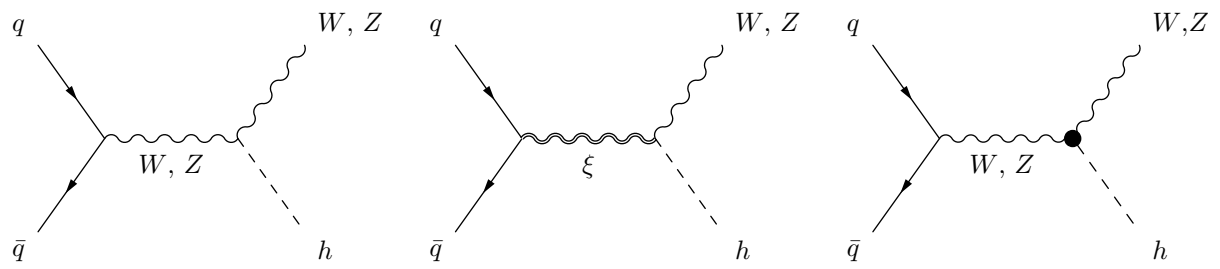

Figure 1. Example diagrams for Vh production in the SM (left), in the vector triplet model (middle), and in the EFT (right), where the blob denotes effects from the dimension-6 operators.

We show the m_{Vh} distributions in the left panels of Fig. 2. While theoretically the m_{Vh} distribution is cleaner, for example when we include initial state radiation, we can see the same effects in the highly correlated $p_{T,V}$ distribution (right panels), due to the simple $2 \to 2$ signal kinematics [10, 11]. The T1 benchmark point is constructed with a low new physics scale and a destructive interference between Standard Model and dimension-6 term. We see that the squared dimension-6 terms are clearly needed to avoid negative cross sections in the high-energy tails of the distributions. Driven by the light new particles, inconsistencies otherwise occur around

$$m_{Vh} > 600 \text{ GeV} \approx \frac{m_\xi^{(\text{T1})}}{2} \qquad \text{or} \qquad p_{T,V} > 300 \text{ GeV} \approx \frac{m_\xi^{(\text{T1})}}{4} \,, \tag{8}$$

clearly within reach of Run II. The reason why differences appear much below $m_{Vh} = m_\xi$ is that the new states are wide and their pole contribution extends through a large interference effect. Because for this benchmark point the discrepancies signal the onset of a new s-channel propagator pole, the agreement between full model and dimension-6 operators is limited and will hardly improve once we include for example dimension-8 terms [19].†

For the constructively interfering benchmark point T4 we observe no dramatic effects in the tails, but the agreement between the full model and the dimension-6 approximation is improved when we include these terms. Both benchmark points therefore suggest to include the dimension-6 squared terms in the LHC analysis, to improve the agreement between the model and the dimension-6 Lagrangian.

WBF Higgs production

Weak-boson-fusion Higgs production is a $2 \to 3$ process with two t-channel gauge bosons carrying the momentum to the Higgs vertex, see Fig. 3. The relevant kinematic variables are the two virtualities of the weak bosons. Following many studies in the framework of the effective W approximation [20, 21] it is straightforward to link them to the p_T of the tagging jets, which even for multiple jet radiation can be linked to the transverse momentum of the Higgs [22] (even though it is not clear if this distribution is theoretically or experimentally favored). Again, we start with the parton-level signal process

$$ud \to u'd'h \tag{9}$$

† We are convinced that, if the LHC experiments should observe such a new resonance, the justification of a dimension-6 description will most likely not be of experimental or theoretical concern.

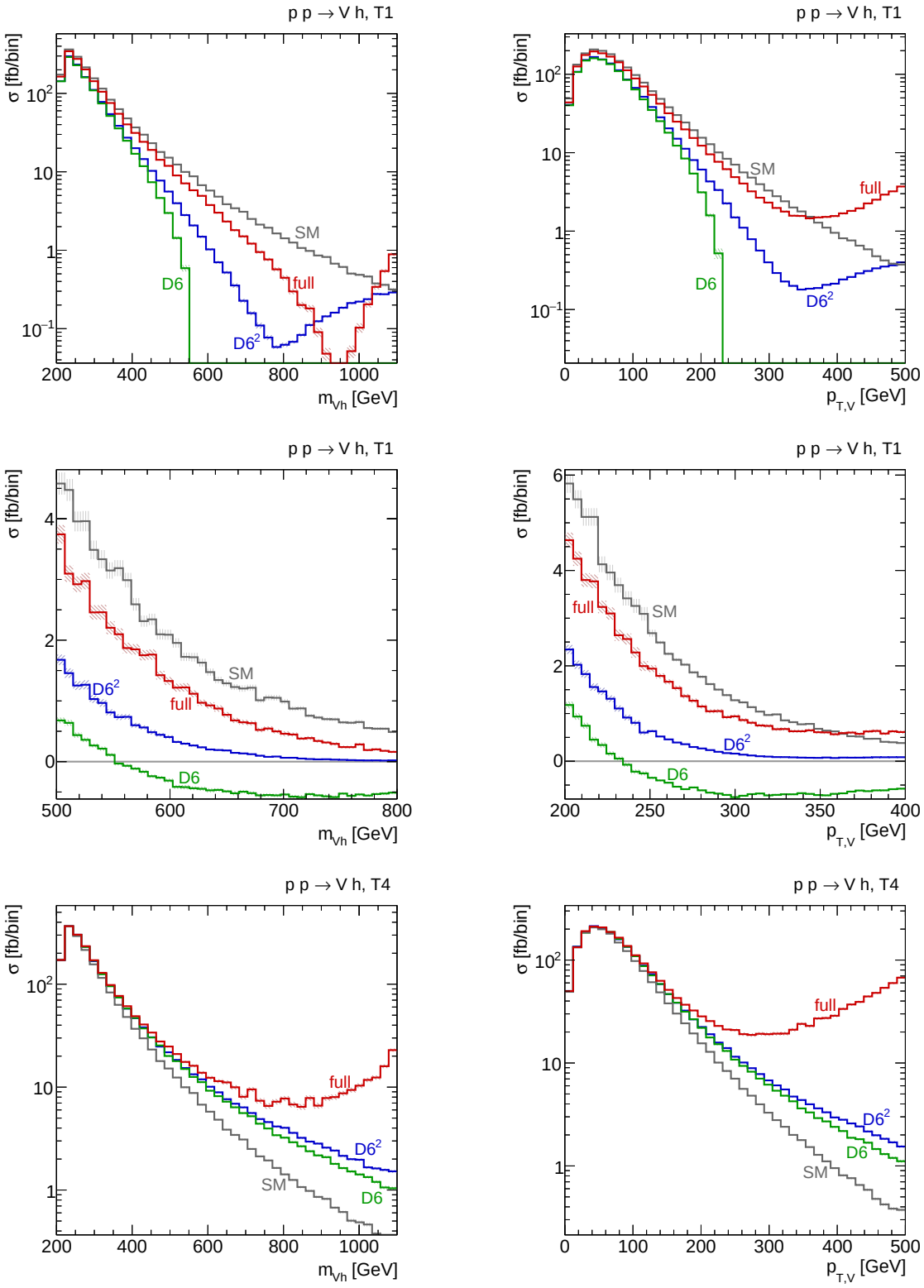

Figure 2. Vh distributions with ("D6^2") and without ("D6") the dimension-6 squared term. The left panels show m_{Vh}, the right panels $p_{T,V}$. The central panels show the region where leaving out the squared dimension-6 terms leads to a negative cross section.

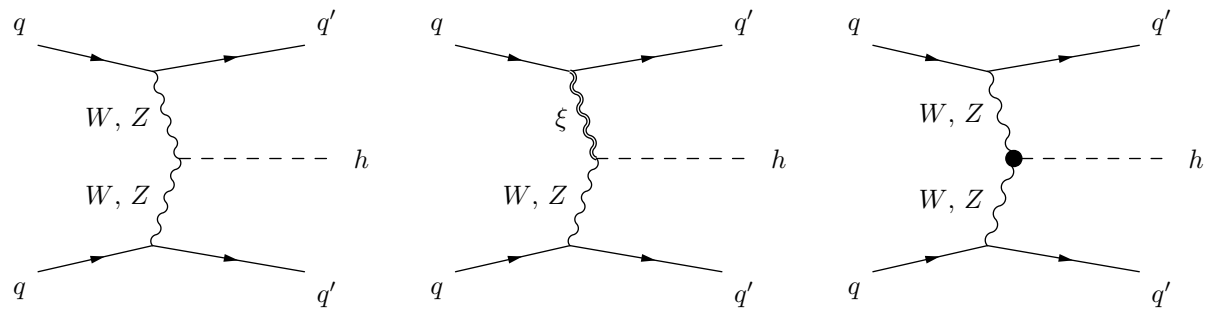

Figure 3. Example diagrams for WBF Higgs production in the SM (left), in the vector triplet model (middle), and in the EFT (right), where the blob denotes effects from the dimension-6 operators.

with only one minimal cut $p_{T,j} > 20$ GeV for the two tagging jets. We show the results for the now constructively interfering benchmark point T1 and the now destructively interfering benchmark point T4 in Fig. 4. Negative event rates for T4 appear around

$$p_{T,j_1} > 600 \text{ GeV} \approx \frac{m_\xi^{(\text{T4})}}{2} \,, \tag{10}$$

forcing us to either disregard the corresponding model hypothesis or to add the dimension-6 squared term. For the less critical point T1 the agreement between the vector triplet model and its dimension-6 approximation including the squared terms extends well into the range where deviations from the Standard Model become visible.

In the middle panels of Fig. 4 we see that indeed the $p_{T,h}$ distribution looks almost identical to p_{T,j_1}. Both of them can be traced back to the unobservable virtualities of the weak bosons. Due to the preferred collinear direction of the quark-vector splittings, the W-mediated and Z-mediated diagrams populate very different parton-level phase-space regions, with basically no interference between them. We can thus define the virtuality variable [11, 21]

$$q = \begin{cases} \max\left(\sqrt{|(p_{u'} - p_d)^2|}\,,\, \sqrt{|(p_{d'} - p_u)^2|}\right) & \text{for } W\text{-like phase-space points,} \\ \max\left(\sqrt{|(p_{u'} - p_u)^2|}\,,\, \sqrt{|(p_{d'} - p_d)^2|}\right) & \text{for } Z\text{-like phase-space points,} \end{cases} \tag{11}$$

with the distribution shown in the bottom panels of Fig. 4. Comparing it to $p_{T,h}$ and p_{T,j_1} we see essentially the same behavior. The strong correlation of q with the observable transverse momenta of the leading tagging jet and the Higgs is explicitly shown in Fig. 5.

Finally, we compare expected exclusion limits on the vector triplet in the absence of a signal, based on the full model vs the dimension-6 approach. For the process shown in Eq. (9) we multiply the cross sections with a branching ratio $\text{BR}(h \to 2\ell 2\nu) \approx 0.01$. We disregard non-Higgs backgrounds as well as parton-shower or detector effects. We then count events in two high-energy bins of the p_{T,j_1} distributions, defining a parameter point to be excluded if $S/\sqrt{S+B} > 2$. While this statistical analysis is not designed to be realistic, it illustrates how the validity of our dimension-6 approach affects possible limits. For our limit setting procedure we choose a two-dimensional plane defined by m_ξ versus a universal coupling rescaling c,

$$g_V = 1 \,, \qquad c_H = c \,, \qquad c_F = \frac{g_V^2}{2g^2}\, c \,, \qquad c_{HHVV} = c^2 \,. \tag{12}$$

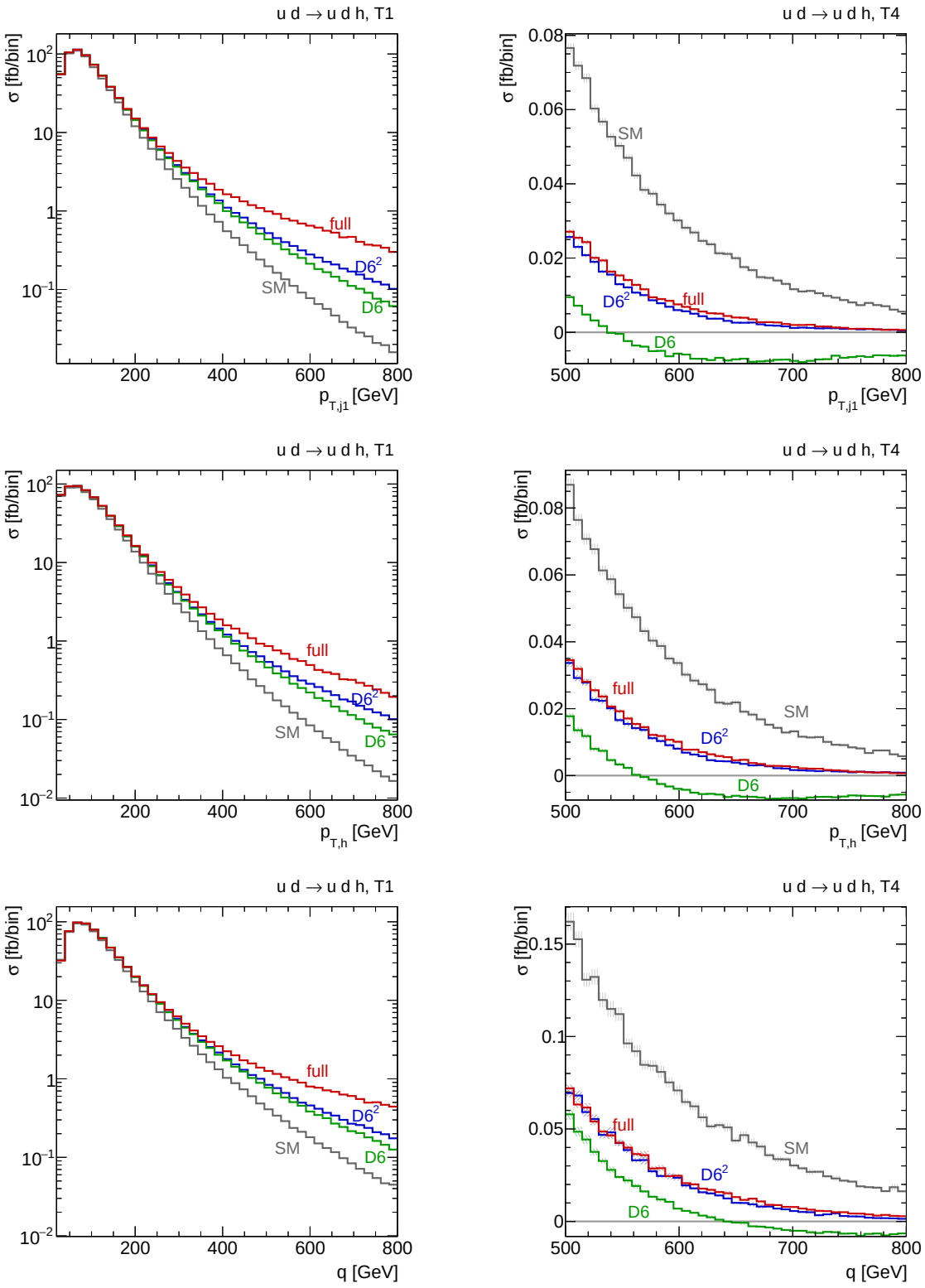

Figure 4. WBF distributions with ("D6^2") and without ("D6") the dimension-6 squared term. From top to bottom: $p_{T,j1}$, $p_{T,h}$, and virtuality q defined in Eq. (11). The right panels show the region where leaving out the squared dimension-6 terms leads to a negative cross section.

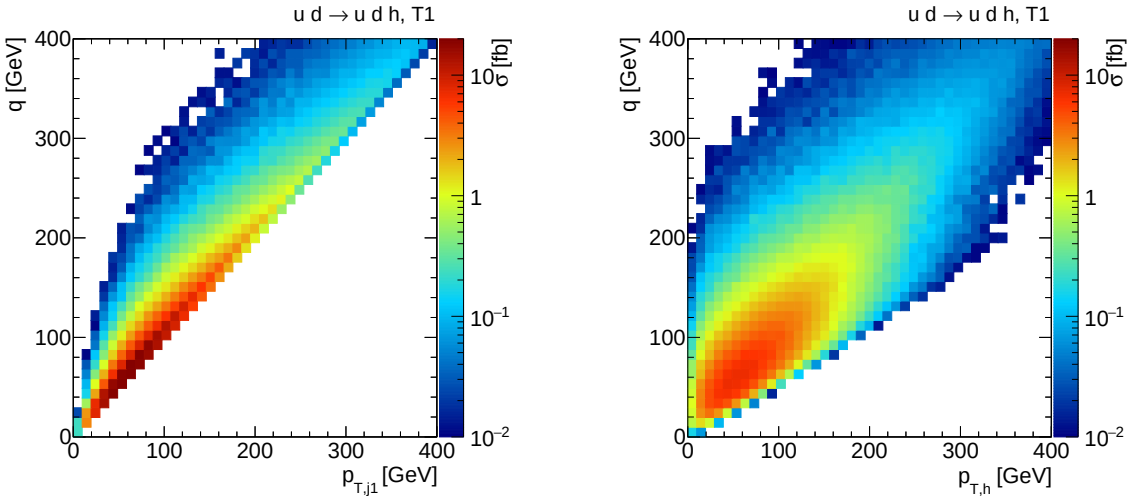

Figure 5. WBF correlations between the virtuality q and p_{T,j_1} (left) or $p_{T,h}$ (right).

This reduces the list of generated dimension-6 operators to

$$f_{WW} = f_{BW} = \frac{c^2}{2g^2} \qquad \text{and} \qquad f_W = -\frac{c^2}{g^2}\,, \tag{13}$$

and all dimension-6 deviations scale like c^2/m_ξ^2. To avoid effects from strongly interacting theories we limit our analysis to $\Gamma_\xi/m_\xi < 1/4$.

In the left panel of Fig. 6 we see that based on event numbers in the range 150 GeV $< p_{T,j_1} <$ 300 GeV, the dimension-6 approximation with the squared terms gives the same limits as the full model, as long as we ensure that the new resonance remains narrow. In the high-energy tail $p_{T,j_1} > 300$ GeV including the squared terms also improves the validity of the dimension-6 approach, but it only leads to identical limits for large m_ξ, combined with strong couplings. Indeed,

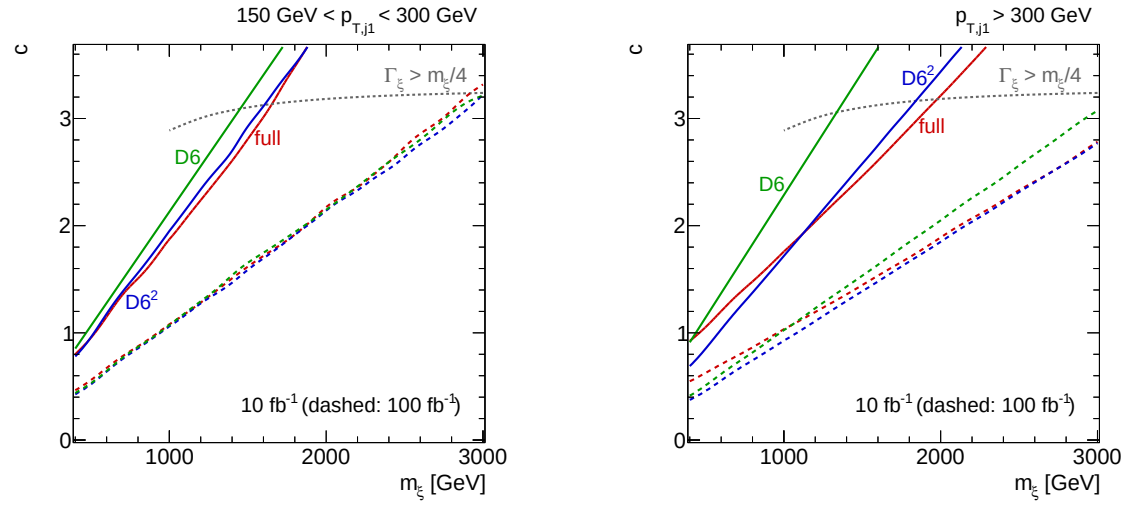

Figure 6. Expected limits on a two-dimensional slice of the vector triplet parameter space. We show the analysis based on the event numbers in 150 GeV $< p_{T,j_1} <$ 300 GeV (left) and based on the tail $p_{T,j_1} > 300$ GeV.

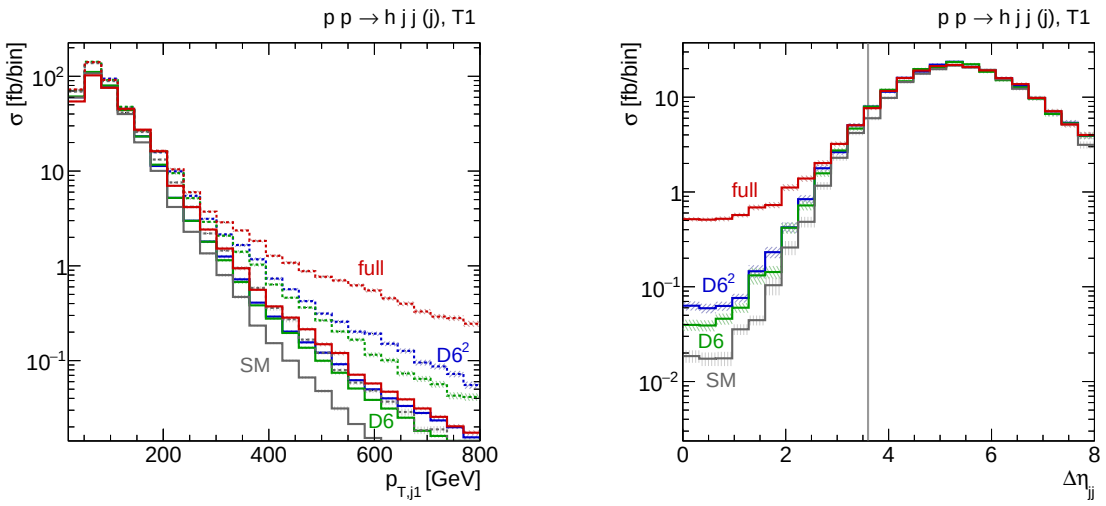

Figure 7. WBF distribution at hadron level. Left: p_{T,j_1} distribution based on the full process, the dashed lines show the distributions based on WBF diagrams only and without a $\Delta\eta_{jj}$ cut. Right: $\Delta\eta_{jj}$ based on WBF diagrams only, the vertical line marks the standard WBF cut following Eq. (15).

limiting the momentum transfer of events for example through an upper limit on $p_{T,j}$ is well known to reduce the dependence on model assumptions [23, 24].

Just as for the Vh production process, at least as long as the event numbers remain small the square of the dimension-6 operators always improves the agreement with the full theory in weak boson fusion. With improved statistics the differences become smaller and ultimately negligible, and the question of whether the squared dimension-6 amplitudes should be taken into account is rendered irrelevant.

Realistic tagging jets

Before we attempt to further improve the description of the full vector triplet model for example in the benchmark point T1, we briefly test if the parton-level effects described above survive a realistic environment. We add a parton shower and jet reconstruction now for the full process

$$pp \to h\, jj\, (+j)\,, \tag{14}$$

simulated in `MadGraph` [18]. Parton showering is performed by `PYTHIA6` [25] using the k_T-jet MLM matching scheme [26] with a minimum k_T jet measure between partons of `xqcut`=20 GeV. `Fastjet` [27] is used to construct jets based on the k_T algorithm with $R = 0.4$. We do not include a Higgs decay because we are only interested in production-side kinematics. The standard WBF cuts then are

$$p_{T,j} > 20 \text{ GeV}\,, \qquad m_{jj} > 500 \text{ GeV}\,, \qquad \Delta\eta_{jj} > 3.6 \tag{15}$$

on the two hardest jets. We veto additional jets with $p_{T,j} > 20$ GeV between these two tagging jets. To analyze the effects of the $\Delta\eta_{jj}$ cut [24], we generate additional samples explicitly excluding Higgs-strahlung diagrams, in spite of the fact that it might break gauge invariance.

In Fig. 7 we show that the distributions are generally robust under parton shower and jet reconstruction, but two complications arise. First, on-shell ξ production contributes to this process and is not entirely removed by the WBF cuts in Eq. (15), leading to visible differences between the

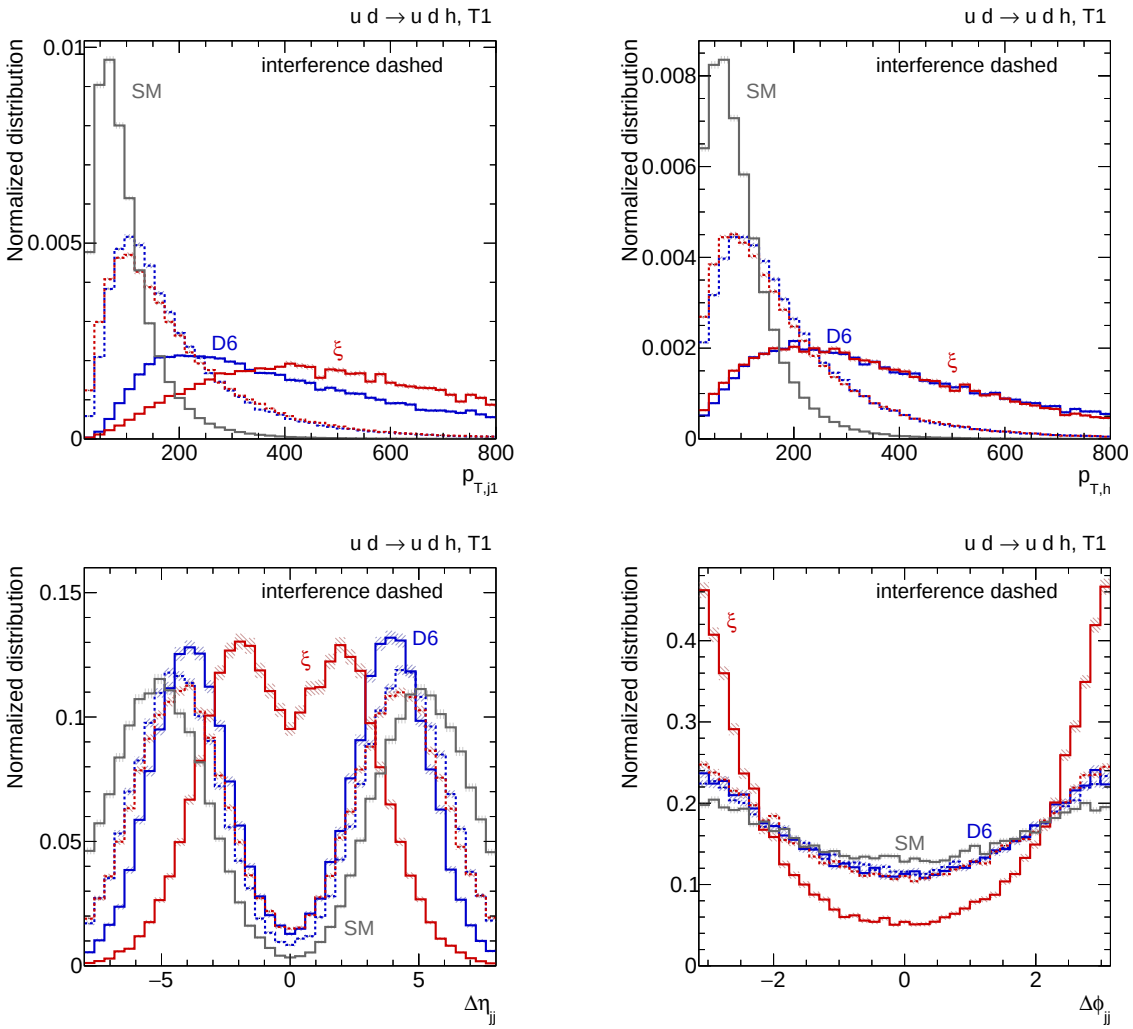

Figure 8. Normalized WBF distributions of the tagging jets. We separate the squared new-physics amplitudes, shown as solid lines, from the interference with the SM-like diagrams (dashed).

full and effective model already at low momenta. Such a resonance peak would be easy to identify experimentally and does not present a major problem for the dimension-6 approximation.

Second, the tension between the full model and the dimension-6 approximation at large momenta now remains below 10 %. This means that the $\Delta\eta_{jj}$ cut not only removes large contributions from Higgs-strahlung–like diagrams, it also gets rid of phase-space regions where the full model and the dimension-6 description differ the most. At the same time, the $\Delta\eta_{jj}$ removes some of its well-known discrimination power for new physics effects versus the Standard Model [24].

III. TOWARDS A SIMPLIFIED MODEL

In the first part of the paper we have shown where in phase space a dimension-6 description of LHC observables breaks down, both for Vh production and for weak boson fusion. For Vh production with its simple $2 \to 2$ kinematics problems are clearly linked to a possible s-channel resonance, as seen in Eq. (8). For weak boson fusion there appears no resonance, but the result of Eq. (10) suggests that the new states in the t-channel have a similar effect. In Fig. 8 we show

different tagging jet distributions, separating the Feynman diagrams including the heavy ξ states. In particular for the critical p_{T,j_1} distribution, the $\Delta\eta_{jj}$ distribution, and the $\Delta\phi_{jj}$ distribution these diagrams are only very poorly described by the dimension-6 approach. In practice this is not a problem because these contributions are strongly suppressed by the heavy mass m_ξ, but it poses the question how we can improve the agreement. The obvious solution to these problems in the s-channel of Vh production and in the t-channel of weak boson fusion is a simplified model [28, 29]. A new vector field mixing with the weak bosons as described by the Lagrangian shown in Eq. (2) is such a simplified model, but its structure is still relatively complex. Obviously, an additional heavy scalar with mass around m_ξ and the appropriate couplings will improve the $2 \to 2$ kinematics for Vh production. The question we want to study in this section is if such a scalar can also improve the weak boson fusion kinematics.

A pseudo-scalar as a simplified vector

The simplest simplified model we can write down includes one new massive scalar S with a Higgs portal and a Yukawa coupling. However, a scalar state will not interfere with the Standard Model diagrams. In analogy to the CP properties of the Goldstone mode contributing to the massive Z boson we define our simplified model with a pseudo-scalar state as

$$\mathcal{L} \supset \frac{1}{2}(\partial_\mu S)^2 - \frac{m_S}{2} S^2 + \sum_{\text{fermions}} g_F \, S\overline{F}\gamma_5 F + g_S \, S^2 \phi^\dagger \phi \,. \tag{16}$$

In Fig. 9 we show the same WBF distributions as in Fig. 8, but including the simplified scalar model. For the $p_{T,j}$ distribution the squared new-physics amplitudes in the full vector model and the simplified scalar model indeed agree well, improving upon the dimension-6 description which breaks down in this distribution. However, the interference term with the Standard Model, which is numerically dominant for most of the distribution and well described in the dimension-6 model, poses a problem. The $\Delta\eta_{jj}$ distributions show even poorer agreement: the spin-1 amplitudes of the Standard Model and the vector triplet have similar phase-space distributions and give two forward tagging jets, while the scalar mediator favors central jets [24]. The $\Delta\phi_{jj}$ distribution, known to be sensitive to the tensor structure of the hard VVh interaction [30], exposes similar differences between the full and simplified model. Altogether, our simplified scalar model with its very different VVh interaction structure does improve the description in the region where the dimension-6 approach breaks down, but it fails to describe interference patterns and angular correlations of the tagging jets.

Splitting functions and equivalence theorem

We can understand this very different behavior of the scalar t-channel mediator as compared to the vector from the splitting kernels in the collinear limit. The matrix element squared for the weak boson fusion process mediated by pseudo-scalars S has the form

$$|\mathcal{M}(qq \to q'q'h)|^2 \propto \frac{g_F^4 \, t_1 t_2}{(t_1 - m_S^2)^2 \, (t_2 - m_S^2)^2} \overset{m_S \to 0}{\longrightarrow} \frac{\text{const}}{t_1 t_2} \,, \tag{17}$$

where t_1 and t_2 denote the respective momentum flow through each scalar propagator. For $m_S \to 0$ the Jacobians from the phase-space integration cancel a possible collinear divergence, while for a light vector boson a soft and a collinear divergence remains. Unlike in the usual WBF process, the tagging jets in our simplified scalar model will not be forward. The reason for this difference in

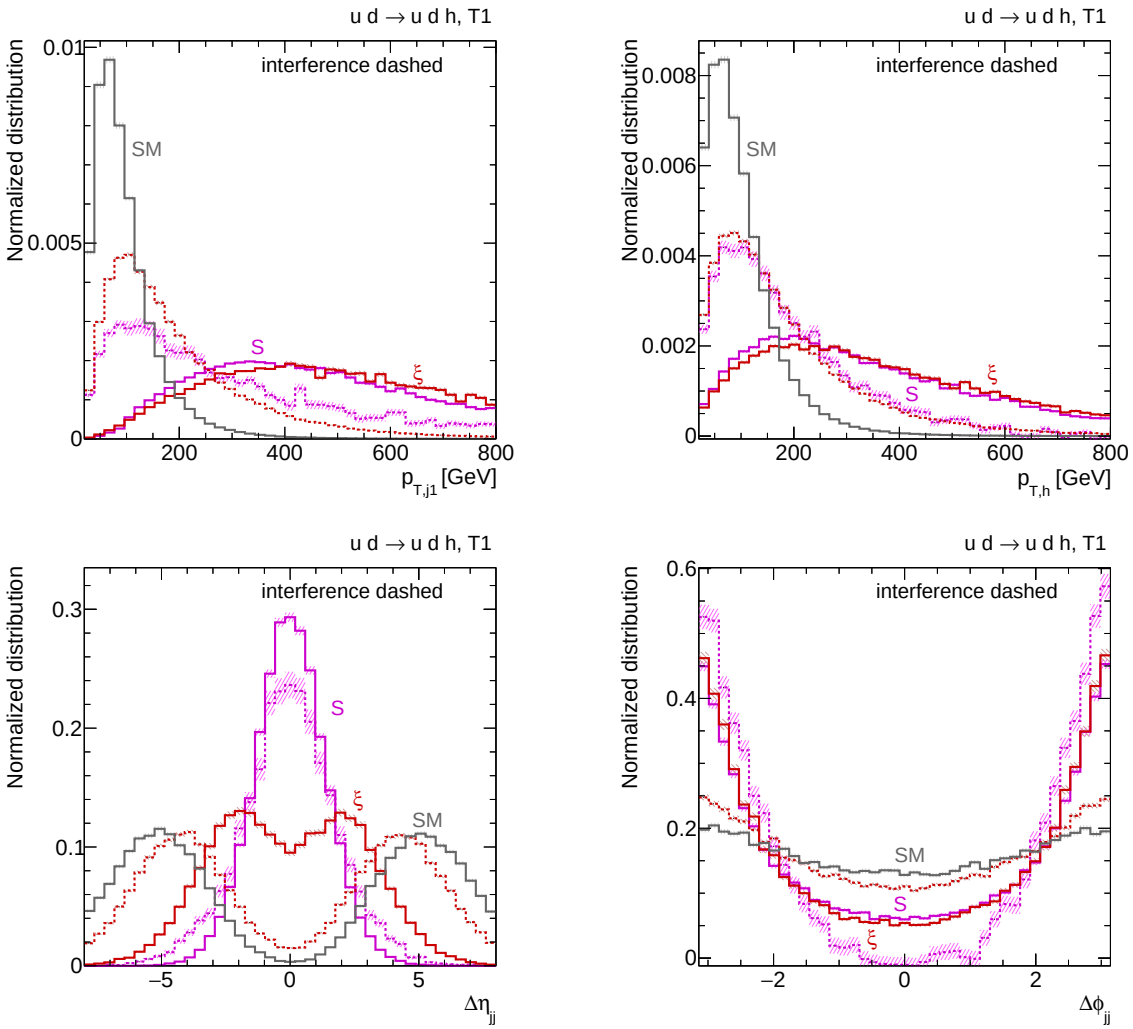

Figure 9. Normalized WBF distributions for a scalar simplified model defined in Eq. (16) vs the vector triplet benchmark.

the infrared is the (pseudo-)scalar coupling to quarks: since the scalar carries no Lorentz index, a $q \to qS$ splitting will be expressed in terms of the momentum combinations $(p_q p'_q)$, $p_q^2 = m_q^2$, and $p_q'^2 = m_q^2$. In the limit of massless quarks only the first term remains as $t = 2(p_q p'_q)$. This factor in the numerator cancels the apparent divergence of the t-channel propagator.

Adding higher-dimensional couplings of the (pseudo-)scalar to fermions, such as

$$\mathcal{L} \supset \sum_{\text{fermions}} \left[g_{F,2} S\overline{F}F + g_{F,3}(\partial_\mu S)\overline{F}\gamma^\mu F + g_{F,4} S(\partial_\mu S)\overline{F}\gamma^\mu\gamma_5 F + g_{F,5} S(\partial_\mu\partial_\nu S)\overline{F}[\gamma^\mu,\gamma^\nu]F \right] , \quad (18)$$

does not change this result qualitatively. After partial integration and using the Dirac equation for the on-shell quarks the coupling $g_{F,3}$ is equivalent to the simple scalar coupling, $g_{F,2} = m_q^2 g_{F,3}$. In the limit of massless quarks, only two of the new structures listed in Eq. (18) contribute at all: $g_{F,2}$ gives exactly the same result as g_F, while $g_{F,5}$ leads to even higher powers of t in the numerator,

$$|\mathcal{M}(qq \to q'q'h)|^2 \propto \frac{g_{F,5}^4\, t_1^3 t_2^3}{(t_1 - m_s^2)^2\,(t_2 - m_s^2)^2} \, . \quad (19)$$

No matter how we couple the (pseudo-)scalar of the simplified model to the external quarks, it never reproduces the collinear splitting kernel of a vector boson.

To be a little more precise, we can write out the spin-averaged matrix element squared for the $q \to q' S$ splitting in terms of the energy of the initial quark E, the longitudinal momentum fraction x, and the transverse momentum p_T, both carried by S,

$$\begin{aligned} |\mathcal{M}(q \to q' S)|^2 &= -2 g_F^2 x m_q^2 + 2 g_F^2 E^2 (1-x) \left[\sqrt{1 + \frac{p_T^2}{E^2 (1-x)^2} + \frac{m_q^2 (1-(1-x)^2)}{E^2 (1-x)^2}} - 1 \right] \\ &= g_F^2 \, \frac{x^2 \, m_q^2}{1-x} + g_F^2 \, \frac{p_T^2}{1-x} + \mathcal{O}\left(\frac{m_q^2 p_T^2}{E^2}, \frac{m_q^4}{E^2}, \frac{p_T^4}{E^2} \right) . \end{aligned} \tag{20}$$

From Eq. (20) one can derive an effective Higgs approximation or *effective scalar approximation* [31]: in the collinear and high-energy limit, a process $qX \to q'Y$ mediated by a (pseudo-)scalar S is described by

$$\sigma(qX \to q'Y) = \int \mathrm{d}x \, \mathrm{d}p_T \, F_S(x, p_T) \, \sigma(SX \to Y) \tag{21}$$

with the splitting function

$$F_S(x, p_T) = \frac{g_F^2}{16\pi^2} \, \frac{x \, p_T^3}{\left(m_S^2 (1-x) + p_T^2 \right)^2} \, . \tag{22}$$

Unlike for vector emission, there is no soft divergence for $x \to 0$. The p_T dependence is the same as for transverse vector bosons [20, 21], as we discuss in some detail in the appendix.

It might seem surprising that our pseudo-scalar is emitted with a fundamentally different phase-space dependence than longitudinal W and Z bosons, in apparent contradiction of the Goldstone boson equivalence theorem. However, the latter only makes a statement about the leading term in an expansion in m_W/E, where $\varepsilon_L^\mu \sim p^\mu / m_W$. At this order the squared matrix element for the splitting $q \to q' W_L$ agrees with the pseudo-scalar result, but is suppressed by a factor of m_q^2/E^2. Higher orders in the m_W/E expansion, outside the validity range of the equivalence theorem, are not suppressed by quark masses. The equivalence theorem is therefore of very limited use in describing the W or Z couplings to quarks except the top.

Which observable to study

Now that it is clear that we cannot further improve the agreement between the vector triplet and its dimension-6 approximation by adding a heavy scalar as a simplified model, we go back to the original problem: how can we best use the dimension-6 approximation for limit setting, and do the shortcomings shown in Fig. 8 harm this approach?

We know that in our LHC analysis we should avoid angular correlations of the tagging jets, like $\Delta\eta_{jj}$ or $\Delta\phi_{jj}$. Instead, we can use momentum-related kinematic variables like

$$x \in \{ q, \, p_{T,j_1}, \, p_{T,j_2}, \, p_{T,h} \} \, . \tag{23}$$

An acceptance cut $x > x_{\min}$ on any of those variables projects out the interesting phase-space regions, while the cut $x < x_{\max}$ ensures the validity of an effective theory description. If $x_{\min} > x_{\max}$ the dimension-6 description is not useful. For each window $x_{\min,\max}$ we can compute the contribution to the theoretical uncertainty

$$\Delta_{\text{theo}}(x_{\min,\max}) = \left| \frac{\sigma_{\text{D6}} - \sigma_{\text{full}}}{\sigma_{\text{full}}} \right| \, , \tag{24}$$

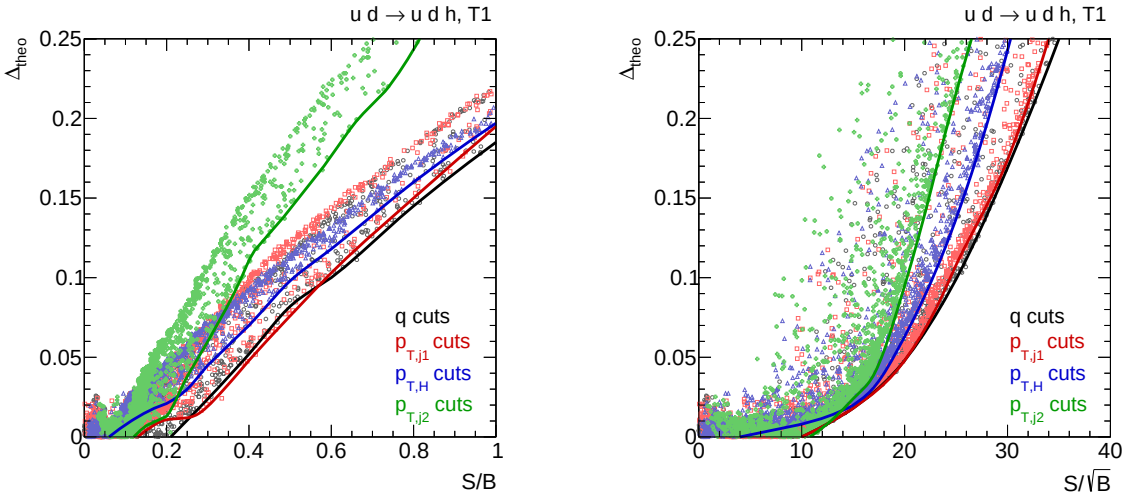

Figure 10. Experimental reach in systematics-driven and statistics-driven channels vs theoretical uncertainties of the dimension-6 description. Each point corresponds to a window $x_{\text{min,max}}$ in one of the four momentum observables that leaves a signal cross section of at least 20 fb.

as well as the statistics-driven and systematics-driven significances

$$\frac{S}{B}(x_{\text{min,max}}) = \left|\frac{\sigma_{\text{full}} - \sigma_{\text{SM}}}{\sigma_{\text{SM}}}\right| \qquad \text{and} \qquad \frac{S}{\sqrt{B}}(x_{\text{min,max}}) = \sqrt{L}\left|\frac{\sigma_{\text{full}} - \sigma_{\text{SM}}}{\sqrt{\sigma_{\text{SM}}}}\right| , \tag{25}$$

where $L = 30$ fb^{-1} is used as a toy number.

The question is for which observable x we find the largest S/B and $S/\sqrt{B}$ values while keeping Δ_{theo} small. In Fig. 10 we show the correlations between theoretical uncertainty and experimental reach for the variables defined in Eq. (23) for a parton-level analysis as defined in Eq. (9). We see that the momentum transfer q or the leading tagging jet's p_{T,j_1} lead to the envelopes with the highest significance for a given theoretical uncertainty Δ_{theo}. This indicates that the leading tagging jet's transverse momentum is the best way of experimentally accessing the momentum flow through the hard process, at least for the hard parton-level process with only two tagging jets.

IV. SUMMARY

While a dimension-6 Higgs analysis at the LHC cannot be considered the leading part of a consistent effective theory, it describes the effects of weakly interacting extensions of the Higgs-gauge sector very well [9]. In this brief study we have answered two practical question concerning such a dimension-6 analysis for Run II.

First, a priori it is not clear if squared dimension-6 terms should be included in calculations. We have studied two particularly challenging parameter points of a vector triplet model for Vh production and for weak-boson-fusion Higgs production. For both processes we find that the dimension-6 squared term avoids negative rate predictions in the m_{Vh} or $p_{T,V}$ distributions of Vh production and in the p_{T,j_1} distribution of weak boson fusion. Even for cases with a constructive interference between the dimension-6 and the Standard Model contributions, it turns out that including the dimension-6 squared term improves the agreement of kinematic distributions between the full model and the dimension-6 approximation. Ultimately, this translates into a better agreement in the expected exclusion limits, and similar conclusions in a different framework have recently been published in Ref. [11].

Second, we have attempted to improve the agreement between the full model and our approximation by using a simplified model. The only significantly simpler model than a mixing gauge extension is an extended scalar sector. While the corresponding deviations between the full model and the dimension-6 approximation are phenomenologically hardly relevant, we find that such an additional scalar improves the modelling of kinematic distributions of the kind m_{Vh} and p_{T,j_1} where the dimension-6 description breaks down. However, this comes at the cost of significant deviations in the dominant interference terms. Moreover, once we include angular correlations like $\Delta\eta_{jj}$ or $\Delta\phi_{jj}$ in weak boson fusion, the simplified model fails badly. The difference can be traced to the divergence structure of the corresponding splittings.

Seeing that the dimension-6 approach is still the better simple model to describe new physics in WBF distributions, we have finally analyzed which phase-space regions provide an interesting window to new physics while being well described by the dimension-6 approximation. We have demonstrated that the leading tagging jet's p_T distribution is particularly suited for such a search for new physics.

Acknowledgments

We would like to thank Torben Schell for very useful discussions and Michael Krämer for his encouragement and support. Moreover, we are grateful to David Lopez-Val and Ayres Freitas, whose inexhaustible energy prepared the ground for this study. All authors acknowledge support from the German Research Foundation (DFG) through the Forschergruppe 'New Physics at the Large Hadron Collider' (FOR 2239), J. B. also through the Graduiertenkolleg 'Particle physics beyond the Standard Model' (GRK 1940).

Appendix A: Effective scalar approximation

In Sec. III we have introduced a pseudo-scalar in the t-channel of weak boson fusion to describe some of the features which we find in the full vector triplet model and which our dimension-6 description does not describe well. In this appendix we collect some of the main formulas and compare the kinematics of fermions radiating scalars, transverse, or longitudinal gauge bosons. Our formalism follows the effective W approximation [20] as well as the effective Higgs approximation [31] and allows us to analytically describe the soft and collinear behavior. If we do not need to describe interference terms with SM gauge bosons we can start with a CP-even scalar splitting $q \to qS$, in terms of the energy of the initial quark E, the longitudinal momentum fraction x, carried by S, and the scalar's transverse momentum p_T:

$$\begin{aligned}
|\mathcal{M}(q \to q'S)|^2 &= 2g_F^2(2-x)m_q^2 + 2g_F^2E^2(1-x)\left[\sqrt{1+\frac{p_T^2}{E^2(1-x)^2}+\frac{m_q^2(1-(1-x)^2)}{E^2(1-x)^2}}-1\right] \\
&= g_F^2\left(4+\frac{x^2}{1-x}\right)m_q^2 + g_F^2\frac{p_T^2}{1-x} + \mathcal{O}\left(\frac{m_q^2p_T^2}{E^2}, \frac{m_q^4}{E^2}, \frac{p_T^4}{E^2}\right) . \qquad \text{(A1)}
\end{aligned}$$

The main feature of this splitting is that the infrared behavior is different for the term proportional to the quark mass and for the surviving term in the realistic limit $m_q \to 0$: in the absence of a fermion mass the collinear divergence from a t-channel propagator is cancelled by the coupling structure. If the term proportional to m_q dominates there will be the usual collinear divergence once we include a scalar propagator. For a pseudo-scalar the structure shown in Eq. (20) is very

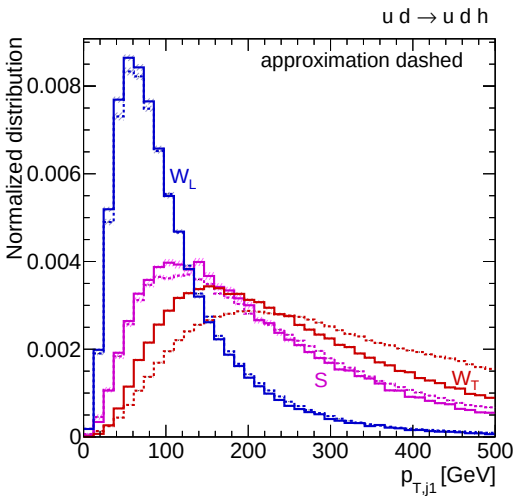

Figure 11. Normalized WBF distributions of the tagging jets in the SM with a heavy Higgs, $m_h = 1$ TeV. Scalar mediators are compared to longitudinal and transverse W bosons following Ref. [21]. The dotted lines give the corresponding predictions of the effective W and scalar approximations, Eq. (A3).

similar,

$$\begin{aligned} |\mathcal{M}(q \to q' S)|^2 &= -2g_F^2 x m_q^2 + 2g_F^2 E^2 (1-x) \left[\sqrt{1 + \frac{p_T^2}{E^2(1-x)^2} + \frac{m_q^2(1-(1-x)^2)}{E^2(1-x)^2}} - 1 \right] \\ &= g_F^2 \, \frac{x^2 \, m_q^2}{1-x} + g_F^2 \, \frac{p_T^2}{1-x} + \mathcal{O}\left(\frac{m_q^2 p_T^2}{E^2}, \frac{m_q^4}{E^2}, \frac{p_T^4}{E^2} \right) . \end{aligned} \tag{A2}$$

In the limit $m_q \to 0$ we can compute universal splitting kernels including only the leading term in p_T, as defined in Eq. (21). Obviously, the scalar and pseudoscalar case given in Eq. (22) are identical, and we can compare them with the splitting kernels for longitudinal or transverse W bosons [20],

$$\begin{aligned} F_S(x, p_T) &= \frac{g_F^2}{16\pi^2} \, x \, \frac{p_T^3}{\left(m_S^2(1-x) + p_T^2\right)^2} , \\ F_T(x, p_T) &= \frac{g^2}{16\pi^2} \, \frac{1+(1-x)^2}{x} \, \frac{p_T^3}{\left(m_W^2(1-x) + p_T^2\right)^2} , \\ F_L(x, p_T) &= \frac{g^2}{16\pi^2} \, \frac{(1-x)^2}{x} \, \frac{2 m_W^2 \, p_T}{\left(m_W^2(1-x) + p_T^2\right)^2} . \end{aligned} \tag{A3}$$

In Fig. 11 we show how these different splittings translate into WBF distributions and compare full simulations in `MadGraph` to the predictions of Eq. (A3). A heavy Higgs, $m_h = 1$ TeV, is needed to guarantee a large energy scale $E \sim m_h \gg p_T \sim m_W, m_S$. In this case we find that the effective scalar approximation quite accurately describes the transverse momentum distribution of the tagging jets. For $m_h = 125$ GeV the assumption of on-shell W bosons or scalars breaks down and the effective descriptions lose their validity.

[1] P. W. Higgs, Phys. Lett. **12**, 132 (1964); P. W. Higgs, Phys. Rev. Lett. **13**, 508 (1964); F. Englert and R. Brout, Phys. Rev. Lett. **13**, 321 (1964).

[2] G. Aad *et al.* [ATLAS Collaboration], Phys. Lett. B **716**, 1 (2012); S. Chatrchyan *et al.* [CMS Collaboration], Phys. Lett. B **716**, 30 (2012).

[3] D. E. Morrissey, T. Plehn and T. M. P. Tait, Phys. Rept. **515**, 1 (2012).

[4] S. Weinberg, Phys. Lett. B **91**, 51 (1980); S. R. Coleman, J. Wess and B. Zumino, Phys. Rev. **177**, 2239 (1969); C. G. Callan, Jr., S. R. Coleman, J. Wess and B. Zumino, Phys. Rev. **177**, 2247 (1969).

[5] C. J. C. Burges and H. J. Schnitzer, Nucl. Phys. B **228**, 464 (1983); C. N. Leung, S. T. Love and S. Rao, Z. Phys. C **31**, 433 (1986); W. Buchmüller and D. Wyler, Nucl. Phys. B **268**, 621 (1986); W. Kilian, Springer Tracts Mod. Phys. **198**, 1 (2003).

[6] C. Englert, A. Freitas, M. M. Mühlleitner, T. Plehn, M. Rauch, M. Spira and K. Walz, J. Phys. G **41**, 113001 (2014).

[7] T. Corbett, O. J. P. Éboli, D. Gonçalves, J. Gonzalez-Fraile, T. Plehn and M. Rauch, JHEP **1508**, 156 (2015).

[8] C. Arnesen, I. Z. Rothstein and J. Zupan, Phys. Rev. Lett. **103**, 151801 (2009); C. Englert and M. Spannowsky, Phys. Lett. B **740**, 8 (2015); M. de Vries, JHEP **1503**, 095 (2015); N. Craig, M. Farina, M. McCullough and M. Perelstein, JHEP **1503**, 146 (2015); S. Dawson, I. M. Lewis and M. Zeng, Phys. Rev. D **91**, 074012 (2015); A. Drozd, J. Ellis, J. Quevillon and T. You, JHEP **1506**, 028 (2015); R. Edezhath, arXiv:1501.00992 [hep-ph]; L. Edelhäuser, A. Knochel and T. Steeger, arXiv:1503.05078 [hep-ph]; M. Gorbahn, J. M. No and V. Sanz, arXiv:1502.07352 [hep-ph];

[9] J. Brehmer, A. Freitas, D. Lopez-Val and T. Plehn, arXiv:1510.03443 [hep-ph].

[10] J. Ellis, V. Sanz and T. You, JHEP **1503**, 157 (2015).

[11] A. Greljo, G. Isidori, J. M. Lindert and D. Marzocca, arXiv:1512.06135 [hep-ph].

[12] L. Berthier and M. Trott, JHEP **1505**, 024 (2015); L. Berthier and M. Trott, JHEP **1602**, 069 (2016); R. Contino, A. Falkowski, F. Goertz, C. Grojean and F. Riva, JHEP **1607**, 144 (2016); O. Bessidskaia Bylund, F. Maltoni, I. Tsinikos, E. Vryonidou and C. Zhang, JHEP **1605**, 052 (2016); F. Maltoni, E. Vryonidou and C. Zhang, arXiv:1607.05330 [hep-ph].

[13] for a different point of view see e. g. C. Englert, R. Kogler, H. Schulz and M. Spannowsky, arXiv:1511.05170 [hep-ph].

[14] I. Low, R. Rattazzi and A. Vichi, JHEP **1004**, 126 (2010); D. Pappadopulo, A. Thamm, R. Torre and A. Wulzer, JHEP **1409**, 060 (2014); A. Thamm, R. Torre and A. Wulzer, Phys. Rev. Lett. **115**, no. 22, 221802 (2015); a FeynRules implementation of the model is available from `http://heidi.pd.infn.it/html/vector/index.html`

[15] J. de Blas, J. M. Lizana and M. Perez-Victoria, JHEP **1301**, 166 (2013); A. Biekoetter, A. Knochel, M. Krämer, D. Liu and F. Riva, Phys. Rev. D **91**, 055029 (2015); A. E. C. Hernández, C. O. Dib and A. R. Zerwekh, arXiv:1506.03631 [hep-ph].

[16] K. Hagiwara, S. Ishihara, R. Szalapski and D. Zeppenfeld, Phys. Rev. D **48**, 2182 (1993).

[17] U. Baur, T. Plehn and D. L. Rainwater, Phys. Rev. D **69**, 053004 (2004).

[18] J. Alwall *et al.*, JHEP **1407**, 079 (2014).

[19] W. Kilian, T. Ohl, J. Reuter and M. Sekulla, Phys. Rev. D **91**, 096007 (2015).

[20] S. Dawson, Nucl. Phys. B **249**, 42 (1985); G. L. Kane, W. W. Repko and W. B. Rolnick, Phys. Lett. B **148**, 367 (1984); J. Alwall, D. Rainwater and T. Plehn, Phys. Rev. D **76**, 055006 (2007); P. Borel, R. Franceschini, R. Rattazzi and A. Wulzer, JHEP **1206**, 122 (2012).

[21] J. Brehmer, J. Jaeckel and T. Plehn, Phys. Rev. D **90**, no. 5, 054023 (2014).

[22] M. Buschmann, C. Englert, D. Gonçalves, T. Plehn and M. Spannowsky, Phys. Rev. D **90**, no. 1, 013010 (2014).

[23] K. Hagiwara, Q. Li and K. Mawatari, JHEP **0907**, 101 (2009);

[24] C. Englert, D. Gonçalves-Netto, K. Mawatari and T. Plehn, JHEP **1301**, 148 (2013); A. Djouadi, R. M. Godbole, B. Mellado and K. Mohan, Phys. Lett. B **723**, 307 (2013).

[25] T. Sjostrand, S. Mrenna and P. Z. Skands, JHEP **0605**, 026 (2006).

[26] M. L. Mangano, M. Moretti, R. Pittau, Nucl. Phys. **B632**, 343-362 (2002).

[27] M. Cacciari, G. P. Salam and G. Soyez, JHEP **0804**, 063 (2008); M. Cacciari, G. P. Salam and G. Soyez, Eur. Phys. J. C **72**, 1896 (2012).

[28] D. Alves *et al.* [LHC New Physics Working Group Collaboration], J. Phys. G **39**, 105005 (2012).
[29] M. J. Dolan, J. L. Hewett, M. Krämer and T. G. Rizzo, arXiv:1601.07208 [hep-ph].
[30] O. J. P. Eboli and D. Zeppenfeld, Phys. Lett. B **495**, 147 (2000); T. Plehn, D. L. Rainwater and D. Zeppenfeld, Phys. Rev. Lett. **88**, 051801 (2002); V. Hankele, G. Klamke, D. Zeppenfeld and T. Figy, Phys. Rev. D **74**, 095001 (2006); M. R. Buckley, T. Plehn and M. J. Ramsey-Musolf, Phys. Rev. D **90**, no. 1, 014046 (2014).
[31] J. R. Ellis, M. K. Gaillard and D. V. Nanopoulos, Nucl. Phys. B **106**, 292 (1976); S. Dawson and L. Reina, Phys. Rev. D **57**, 5851 (1998); E. Braaten and H. Zhang, arXiv:1510.01686 [hep-ph].